Quaternary International 358 (2015) 160–170

Contents lists available at ScienceDirect

Quaternary International

journal homepage: www.elsevier.com/locate/quaint

Comparison of monthly precipitation derived from high-resolution gridded datasets in arid Xinjiang, central Asia

Xiaofan Zhu, Mingjun Zhang*, Shengjie Wang, Fang Qiang, Ting Zeng, Zhengguo Ren, Lei Dong

College of Geography and Environmental Science, Northwest Normal University, Lanzhou 730070, China

ARTICLE INFO

Article history:
Available online 3 January 2015

Keywords:
Xinjiang
Gridded precipitation
Arid central Asia

ABSTRACT

To investigate the reliability of global gridded precipitation datasets with horizontal resolution of 0.5° × 0.5° in arid Xinjiang, central Asia, the monthly precipitation datasets released by the Climatic Research Unit (CRU TS, version 3.21), the University of Delaware (Terrestrial Precipitation: 1900–2010 Gridded Monthly Time Series, version 3.01), the Global Precipitation Climatology Centre (GPCC Full Data Reanalysis Product, version 6) and the National Oceanic and Atmospheric Administration (NOAA's Precipitation Reconstruction over Land) during 1979–2010 were selected. A precipitation dataset released by the National Meteorological Information Center, China Meteorological Administration is applied as the observation series. The result indicates that changes in seasonal and annual precipitation can be simulated by the four gridded datasets in most regions of Xinjiang, but there are seasonal and regional discrepancies in the correlation coefficients (R), mean bias error (MBE) and root-mean-square error (RMSE). Generally speaking, the gridded datasets can be more effective in simulating precipitation in low-lying basins, that is, the elevation is less than 1500 m (mainly desert and scattered oasis), while RMSE in mountainous areas is much larger than that in low-lying areas. In Altay, Tianshan and Kunlun Mountains, the precipitation simulated by the gridded datasets is less than that of observation series. The accuracy of gridded precipitation datasets generally decreases with elevation. On a seasonal basis, the errors of gridded precipitation datasets in summer months are generally higher than those in other seasons, and RMSE usually shows low values during wintertime. Among the four gridded precipitation datasets, RMSE of CRU is slightly larger than other three datasets in most areas of Xinjiang. The wetting trend magnitude in this study area from 1979 to 2010 is generally underrated by all the gridded datasets, indicating that the long-term precipitation trend using gridded datasets should be treated with caution.

1. Introduction

Precipitation plays a vital role in the global energy and water cycles. During recent decades, frequent natural hazards (e.g. flash flood, rainstorm, urban waterlogging) related with extreme precipitation events have led to great economic and social loss for humans (Beniston and Stephenson, 2004; Qian et al., 2007; Zolina et al., 2010; Shiu et al., 2012). Global and regional precipitation data with high accuracy is widely needed in hydrometeorological forecast and climate change research. In the past several decades, researchers have made great efforts to acquire high-resolution gridded precipitation datasets by interpolation and assimilation from station and/or satellite data (Kistler et al., 2001; Harris et al., 2014; Isotta et al., 2014; Schneider et al., 2014). The widely-applied gridded datasets have provided important information about the distribution and changes of precipitation in a global or regional scale (Takahashi et al., 2006; Bosilovich et al., 2008). However, the inevitable errors of simulated precipitation cannot be totally ignored. The gridded data must be verified according to observations, before they are used for assessing climate change in some specific regions (Janowiak et al., 1998; Silva et al., 2011; Sohn et al., 2012; Sylla et al., 2013; Lin et al., 2014; Tong et al., 2014).

Central Asia is far away from any oceans, and precipitation events in high mountains are much more frequent than that in low-lying basins (Schiemann et al., 2008; Bothe et al., 2012). Xinjiang Uygur Autonomous Region, a remote province in northwestern China, lies in central Asia. The annual precipitation is

* Corresponding author.
E-mail address: mjzhang2004@163.com (M. Zhang).

http://dx.doi.org/10.1016/j.quaint.2014.12.027
1040-6182/

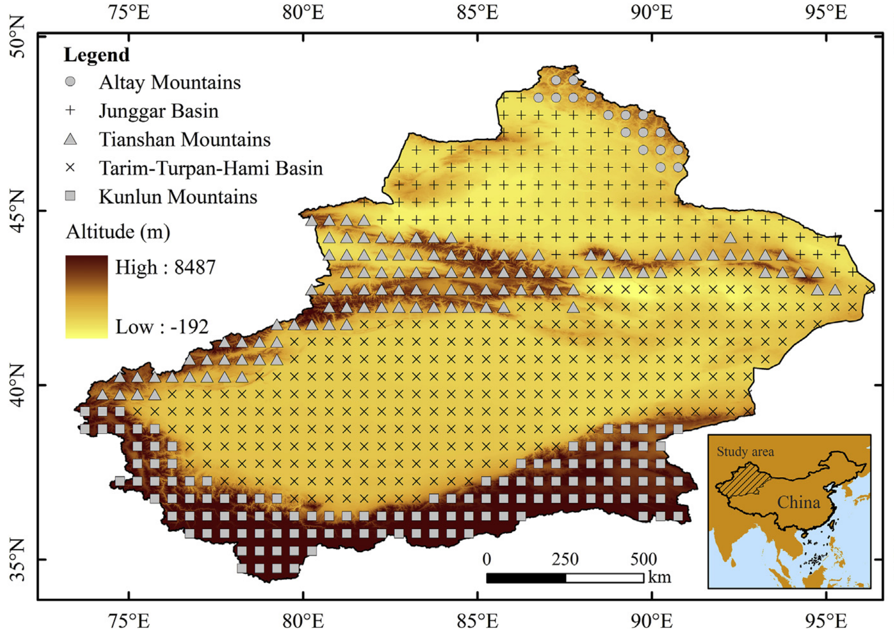

Fig. 1. Distribution of grid boxes with horizontal resolution of 0.5° × 0.5° in Xinjiang, central Asia.

approximately 165.5 mm in Xinjiang, while it is up to 409.1 mm in Tianshan Mountains (Shi et al., 2008). In some desert stations, annual precipitation is less than 10 mm. In this study area, the existing meteorological observation network mainly is concentrated in the oasis belts, and in-situ observations are still scarce in the vast deserts and mountains (e.g. Ling et al., 2012; Xu et al., 2013; Wang et al., 2013a, 2013b, 2014). Only limited station data can be used in interpolation and assimilation, which may reduce the applicability of global gridded datasets for this region. Previous researches showed that the reliability of most global gridded precipitation datasets in eastern China is far better than that in western China, which is related to uneven station distribution and complex topography (Zhao and Fu, 2006; Ma et al., 2009). However, verification of gridded precipitation datasets at resolution no less than 0.5° × 0.5° grids is still limited in arid Xinjiang, and more comparisons on seasonal and annual basis in detail are still needed.

In order to verify the reliability of global gridded precipitation datasets in some specific regions, support of long-term precipitation observations is usually needed. In 2012, a gridded dataset of monthly/daily precipitation at resolution of 0.5° × 0.5° was released by the National Meteorological Information Center, China Meteorological Administration. This dataset is based on the long-term observations and considered to be one of the most important climatological products in China (NMIC, 2012). This real-time

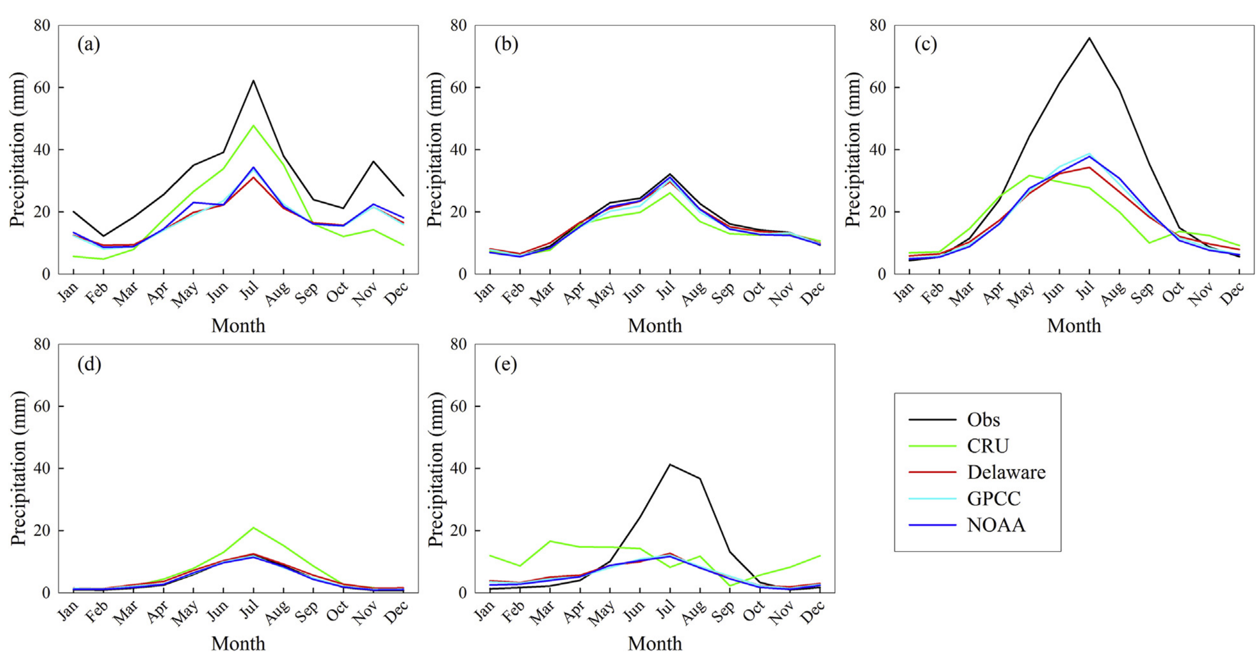

Fig. 2. Monthly mean precipitation in different subregions of Xinjiang derived from gridded datasets and observations during 1979–2010. (a) Altay Mountains; (b) Junggar Basin; (c) Tianshan Mountains; (d) Tarim–Turpan–Hami Basin; (e) Kunlun Mountains.

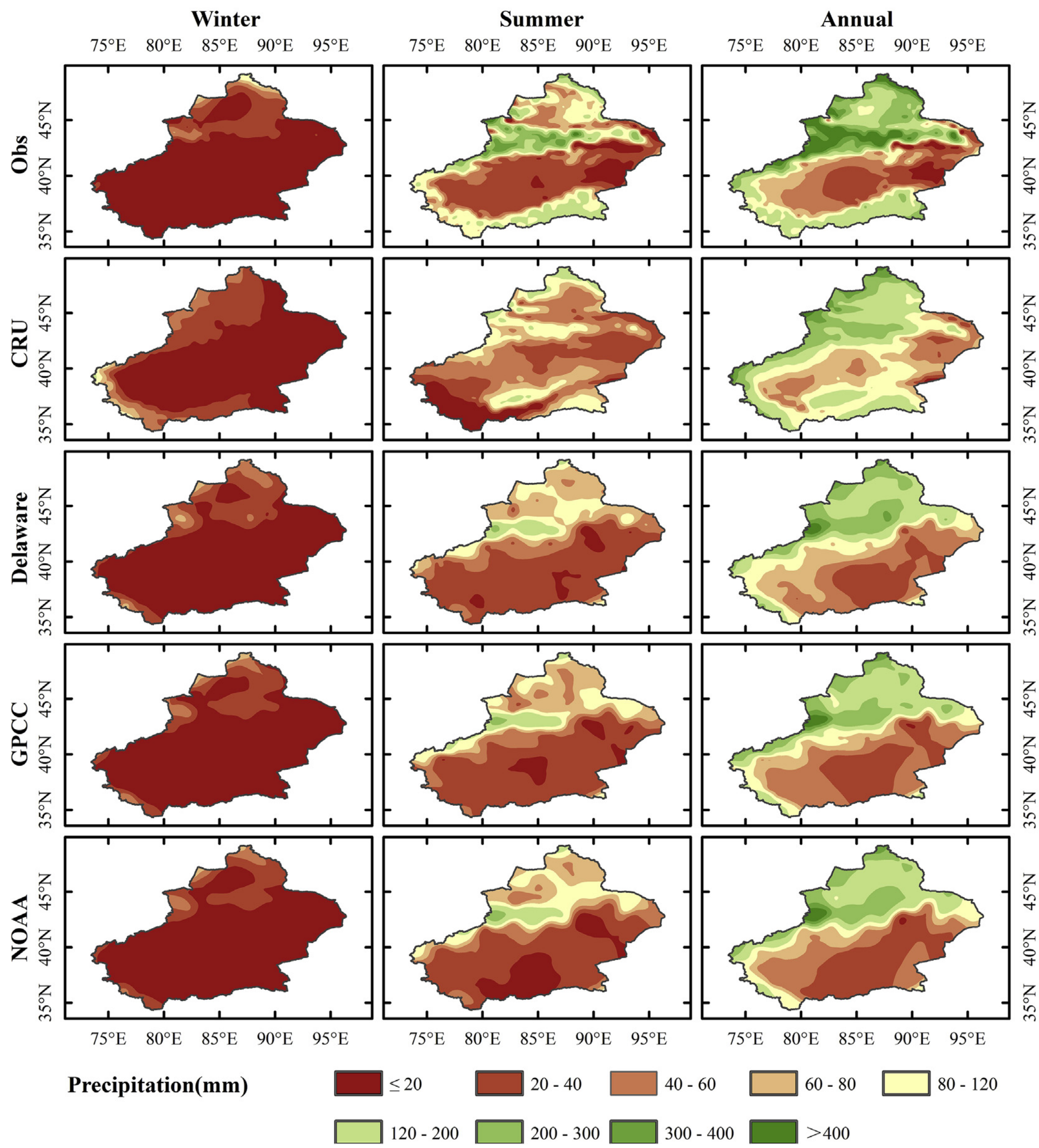

Fig. 3. Spatial distribution of winter precipitation (left column), summer precipitation (middle column) and annual precipitation (right column) derived from gridded datasets and observations in Xinjiang during 1979–2010.

dataset provides a reference series for assessing the applicability of global gridded datasets in arid Xinjiang. In this study, four precipitation datasets released by Climatic Research Unit (CRU), the University of Delaware, the Global Precipitation Climatology Centre (GPCC) and the National Oceanic and Atmospheric Administration (NOAA) with horizontal resolution of 0.5° × 0.5° are selected, and all the selected datasets are applied to the year 2010 in view of the consistency of time series. The spatial–temporal changes in seasonal and annual precipitation derived from these datasets are calculated respectively, and the reliability of these datasets in Xinjiang is discussed.

2. Data and method

2.1. Data sources

2.1.1. Global gridded precipitation datasets

Four datasets of global precipitation with horizontal resolution of 0.5° latitude by 0.5° longitude were selected in this study.

(i) CRU TS version 3.21 (CRU). This dataset is produced by the Climatic Research Unit (CRU), University of East Anglia, England. Station anomalies (1961–1990 means) were spatially interpolated into 0.5° × 0.5° grid boxes covering the global land surface excluding Antarctica, and combined with an existing climatology to obtain absolute monthly values. More details about data interpolation and quality assessment were reported by Harris et al. (2014). The latest version CRU TS version 3.21 (available at http://www.cru.uea.ac.uk/data) covering the period 1901–2012 is applied in this paper.

(ii) Terrestrial Precipitation: 1900–2010 Gridded Monthly Time Series version 3.01 (Delaware). This dataset is produced by the University of Delaware with support from NASA's Innovation in Climate Education (NICE) Program. The station data of monthly precipitation is compiled from several updated sources (e.g. Global Historical Climatology Network (GHCN2)). Climatologically aided interpolation (CAI) (Willmott and Robeson, 1995) is used to estimate the monthly total precipitation fields. Version 3.01 was released

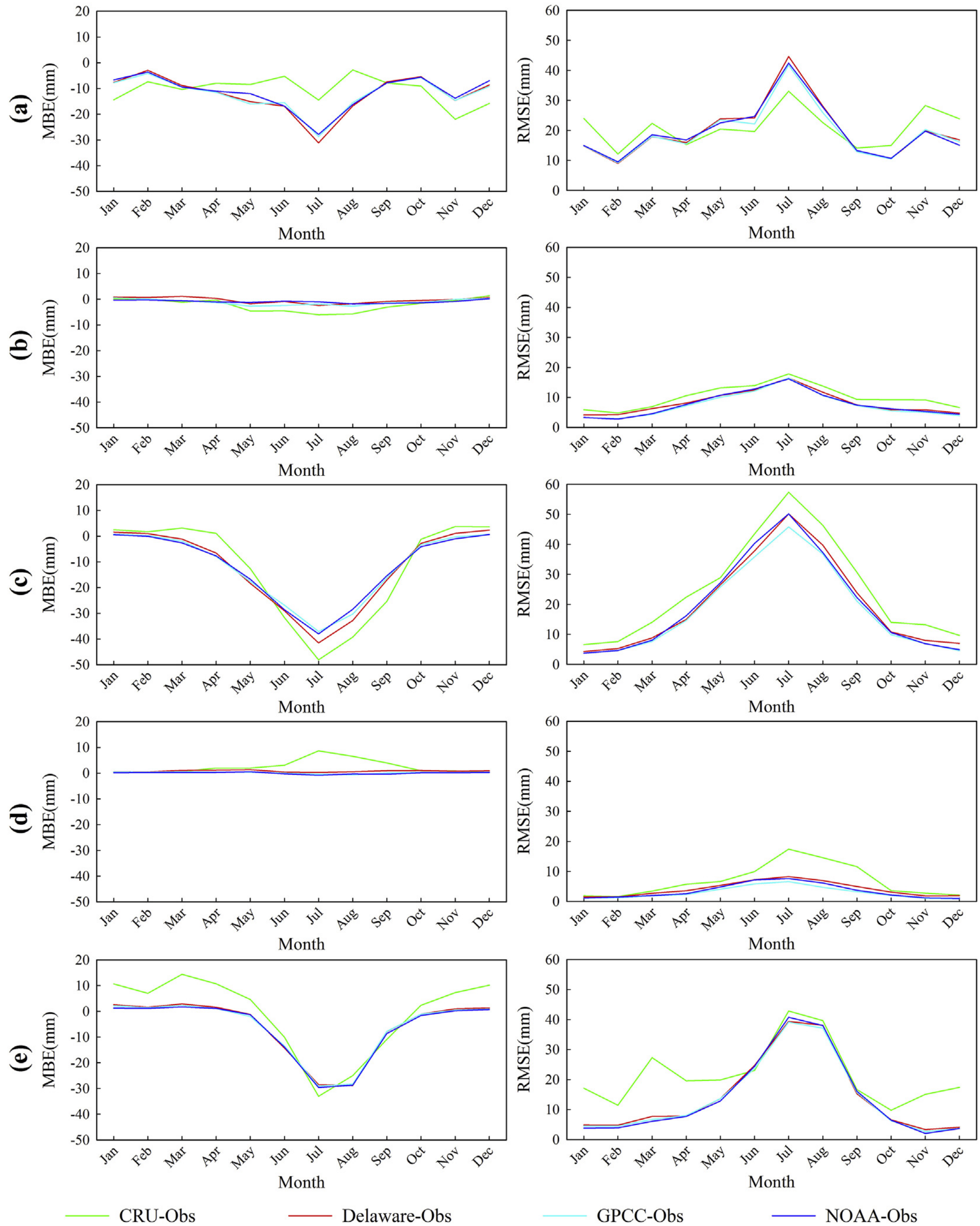

Fig. 4. Monthly mean bias error (MBE, left column) and root-mean-square error (RMSE, right column) of mean precipitation in different subregions of Xinjiang derived from gridded datasets during 1979–2010. (a) Altay Mountains; (b) Junggar Basin; (c) Tianshan Mountains; (d) Tarim–Turpan–Hami Basin; (e) Kunlun Mountains.

on June, 2012, acquirable at http://climate.geog.udel.edu/~climate/.

(iii) Global Precipitation Climatology Centre Full Data Reanalysis Product version 6 (GPCC). It is operated by the Deutscher Wetterdienst (DWD, National Meteorological Service of Germany) as a German contribution to the World Climate Research Programme (WCRP). The quality-controlled data from more than 60,000 world-wide rain gauges is used as background climatology. Data processing and accuracy assessment were presented in Schneider et al. (2014) and Becker et al. (2013). Version 6 covering the period 1901–2010 was released in 2011 (available at http://gpcc.dwd.de).

(iv) NOAA's Precipitation Reconstruction over Land (NOAA). The global monthly precipitation data since 1948 was released by National Oceanic and Atmospheric Administration (NOAA). The dataset was derived from over 17,000 gauges in the Global Historical Climatology Network (GHCN2) and the Climate Anomaly Monitoring System (CAMS) datasets. The optimal interpolation (OI) method of Gandin has been applied to create monthly gridded analyses of the global land precipitation (Chen et al., 2002). The data can be downloaded from NOAA/OAR/ESRL PSD at http://www.esrl.noaa.gov/psd.

The provincial boundary of the Xinjiang Uygur Autonomous Region stretches from 34°19′ 59″ to 49°10′ 42″N and from 73°29′ 11″

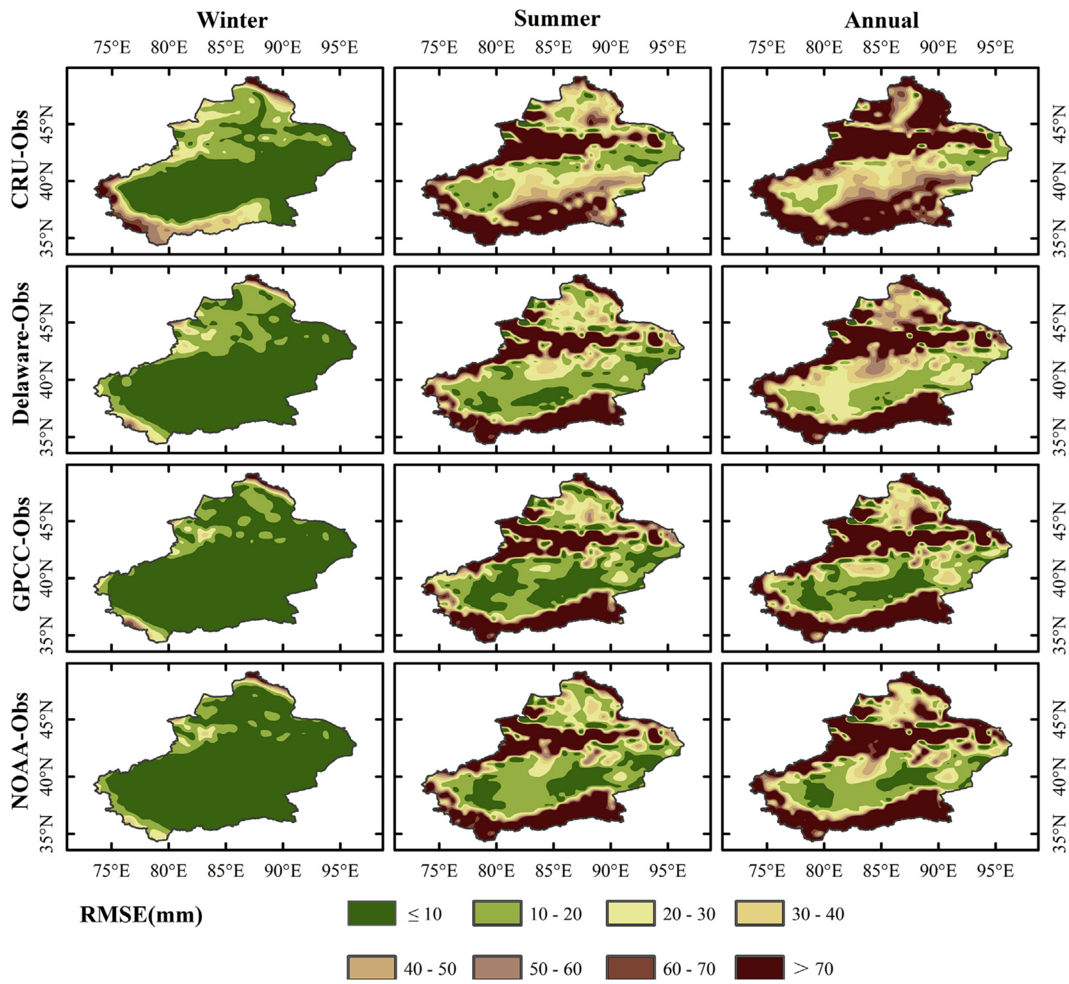

Fig. 5. Spatial distribution of root-mean-square error (RMSE) of winter precipitation (left column), summer precipitation (middle column) and annual precipitation (right column) derived from gridded datasets and observations in Xinjiang during 1979–2010.

to 96°23′ 13″E (Deng et al., 2005), and 699 grids were selected in the study area. Based on the main topography, the study region can be classified into five subregions (Fig. 1), namely, Altay Mountains, Junggar Basin, Tianshan Mountains, Tarim–Turpan–Hami Basin, and Kunlun Mountains from north to south, respectively. The time series from 1979 to 2010 in the datasets is selected in this study.

2.1.2. Dataset of observation precipitation

China Monthly Surface Precipitation 0.5° × 0.5° Gridded Dataset V2.0 (available at http://cdc.cma.gov.cn) is a gridded data released by NMIC (National Meteorological Information Center), China Meteorological Administration (CMA). This dataset consists of monthly surface precipitation with 0.5° × 0.5° horizontal resolution in China since 1961. The latest observed precipitation data from approximate 2400 stations has been spatially interpolated by thin plate spline (TPS) in ANUSPLIN software to generate this dataset. In order to eliminate the influence of elevation on precipitation, a digital elevation model GTOPO30 has been used in spatial interpolation. An assessment report of this dataset shows root-mean-square error (RMSE) ranges between 0.2 and 0.8 mm on a monthly basis, and more information about the calculation procedure is also described by NMIC (NMIC, 2012; Zhao et al., 2014). According to our previous studies (Wang et al., 2013c; Ren et al., 2015), this dataset can describe the spatial and seasonal patterns of precipitation in China. In this study, this dataset is applied as the observation data.

2.2. Method

Two parameters, mean bias error (MBE) and root-mean-square error (RMSE), are applied to quantify the errors of gridded precipitation datasets in this study. The formulas of MBE and RMSE are given as follows:

$$\mathrm{MBE} = \frac{\sum_{i=1}^{n}(P_i - p_i)}{n}, \tag{1}$$

$$\mathrm{RMSE} = \sqrt{\frac{\sum_{i=1}^{n}(P_i - p_i)^2}{n}}, \tag{2}$$

where P_i and p_i are grid-derived and observed precipitation, respectively. For the calculation of correlation coefficients (R), Pearson's correlation coefficients and two-tailed t-test are used. The non-parametric Sen's method (Sen, 1968) is applied to estimate the long-term trend magnitude of precipitation on seasonal and annual basis. The spatial distribution of long-term mean and trend magnitude was processed in ArcGIS 9.3.

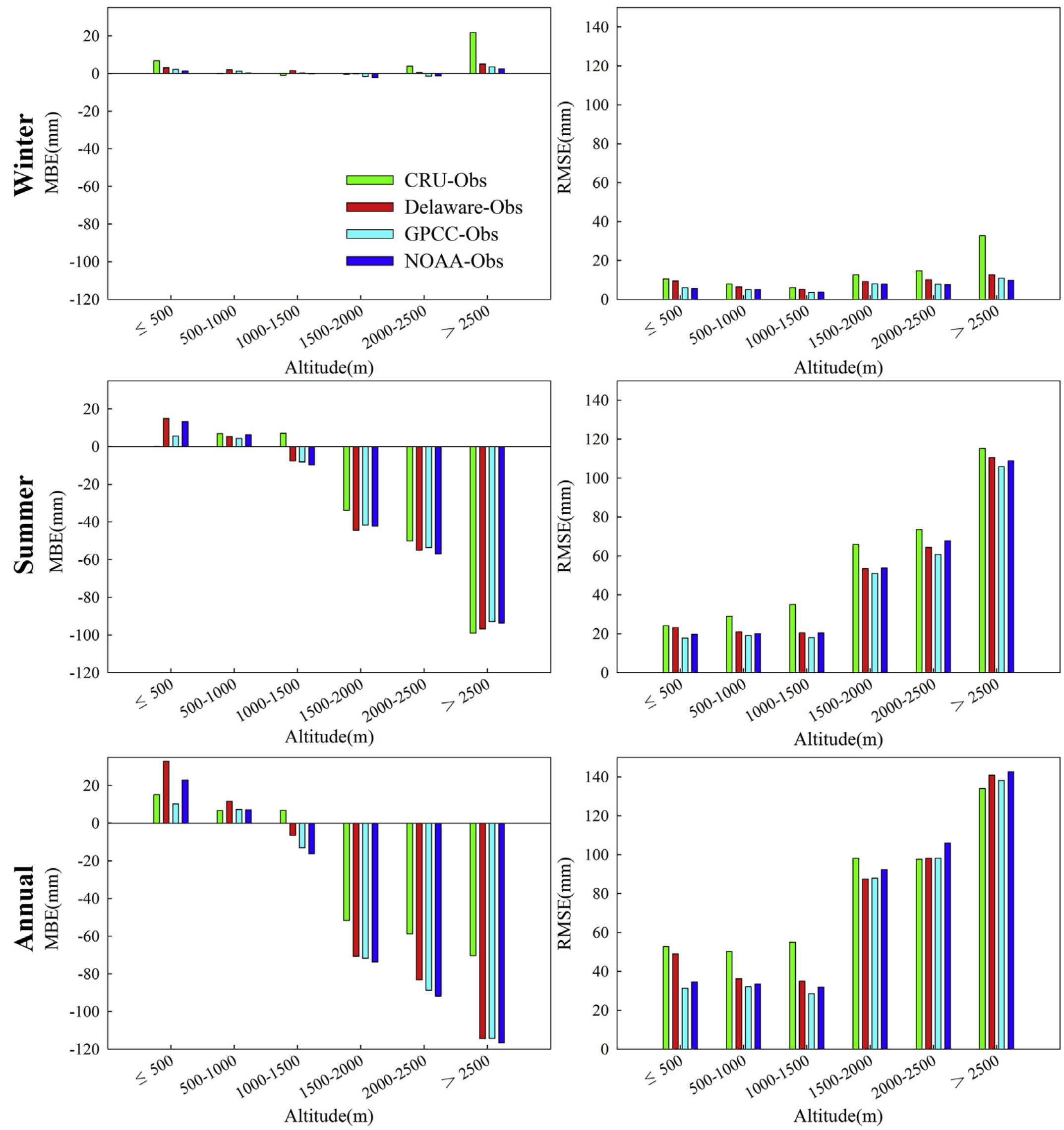

Fig. 6. Variation of mean bias error (MBE) and root-mean-square error (RMSE) of winter precipitation (top), summer precipitation (middle) and annual precipitation (bottom) in different elevation ranges derived from gridded datasets and observations in Xinjiang during 1979–2010.

3. Results

3.1. Comparison of long-term climatology

Fig. 2 demonstrates the variation of monthly precipitation in different subregions of Xinjiang. Precipitation usually concentrates in summer months, which can be seen from all the subregions. Generally, the precipitation peaks in summer are underrated by these global gridded datasets. In Altay (Fig. 2a) and Tianshan Mountains (Fig. 2c), the main summer precipitation peaks can be simulated with gridded datasets, although the peak month derived from CRU in Tianshan Mountains is earlier (May) than that from other three datasets (July). However, in Kunlun Mountains (Fig. 2e), the summer rain peak is greatly smoothed. Compared with mountainous areas, the low-lying basins usually have less precipitation amounts. In Junggar (Fig. 2b) and Tarim–Turpan–Hami Basins (Fig. 2d), the gridded datasets are relatively similar to observations. Among the four gridded datasets, the variation feature derived from Delaware, GPCC and NOAA is generally consistent with each other, while CRU shows obvious difference from other three.

As shown in Fig. 3, spatial diversity of seasonal and annual precipitation exists in Xinjiang. In winter (left column in Fig. 3), the mean precipitation in the northern Xinjiang is more than 20 mm, and the maximum value is in the Altay Mountains. This spatial pattern can be simulated with Delaware, GPCC and NOAA, but the simulated value of precipitation with CRU is higher in Kunlun Mountains and lower in Altay Mountains. In summer (middle column in Fig. 3), the "wet island" of Tianshan Mountains in the middle of Xinjiang can be seen from all the four gridded datasets. However, Delaware, GPCC and NOAA cannot represent precipitation in the Altay and Kunlun Mountains, and CRU also has an underestimated region in southwestern Xinjiang (eastern Kunlun Mountains). For the annual precipitation (right column of Fig. 3), the relatively humid Tianshan Mountains as well as northern Xinjiang can be described by these gridded datasets. However, Delaware, GPCC, and NOAA cannot simulate the precipitation in the Kunlun Mountains. The spatial pattern of the arid

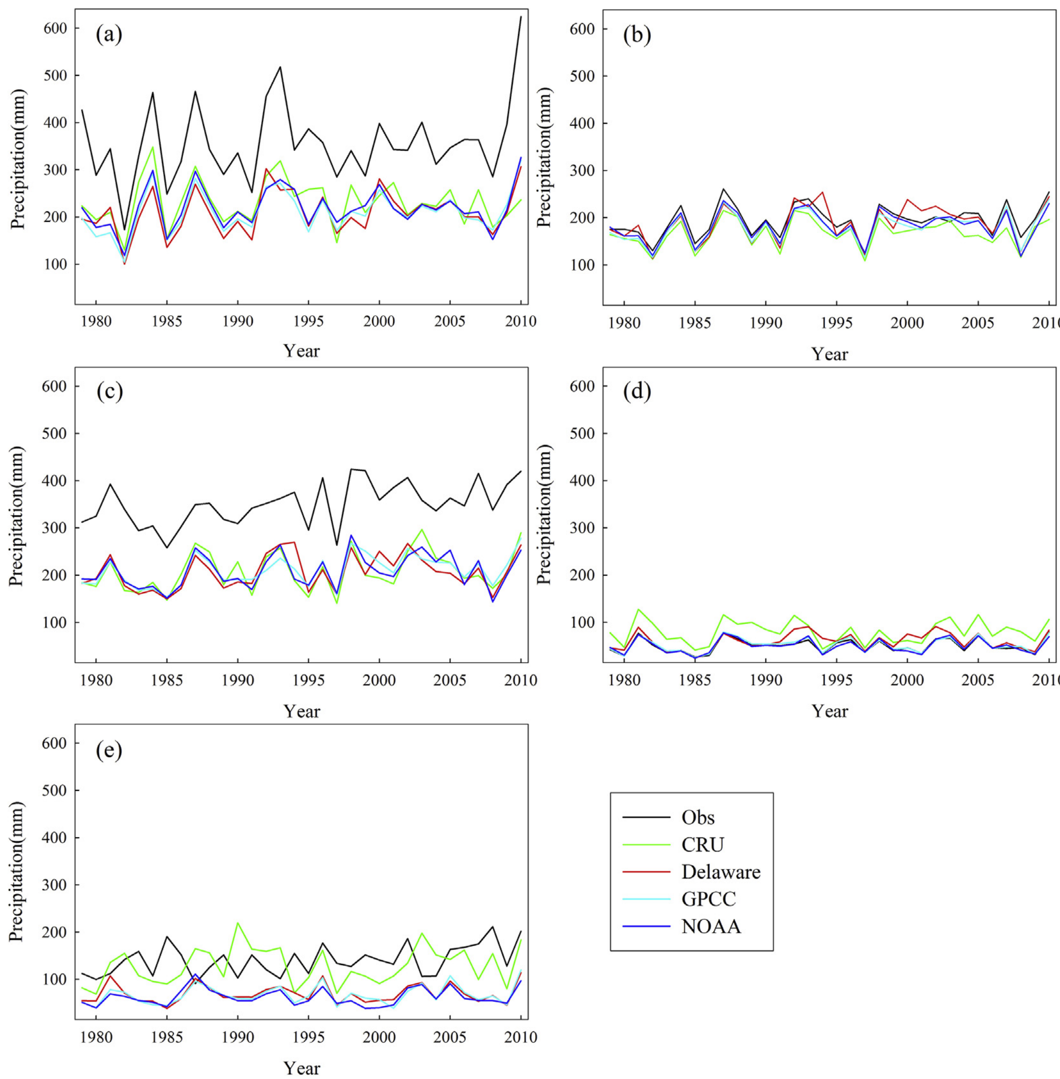

Fig. 7. Interannual changes in mean precipitation in different subregions of Xinjiang derived from gridded datasets and observations during 1979–2010. (a) Altay Mountains; (b) Junggar Basin; (c) Tianshan Mountains; (d) Tarim–Turpan–Hami Basin; (e) Kunlun Mountains.

Tarim–Turpan–Hami Basin flanked by humid mountains can only be found in CRU, although CRU generally makes overestimates in this basin.

3.2. Comparison of errors derived from gridded datasets

Monthly MBE and RMSE of gridded precipitation datasets in Xinjiang are shown in Fig. 4. MBE in Junggar and Tarim–Turpan–Hami Basins is close to 0 mm, especially for GPCC, NOAA and Delaware, indicating a good simulation for these regions (Fig. 4b and d). Specifically, MBE is slightly below 0 mm in Junggar Basin and that in Tarim–Turpan–Hami Basin is slightly above 0 mm. The minimum value of MBE can be found in July (−6.06 mm, for CRU) in Junggar Basin, while the maximum value exists in July (8.67 mm, for CRU) in Tarim–Turpan–Hami Basin. In addition, RMSE in Junggar and Tarim–Turpan–Hami Basins also shows low values within 20 mm, although RMSE is slightly higher in summer and lower in winter. Compared with other three datasets, CRU usually has larger value of RMSE. In three mountainous regions (Fig. 4a, c and e), MBE is usually more negative and RMSE is more positive, compared with that in low-lying basins.

Table 1 shows the correlation coefficients, MBE and RMSE for each gridded precipitation datasets on seasonal and annual basis. In Altay Mountains (Region I in Table 1), the correlation coefficients between CRU and observations exceed 0.7 in spring, summer and autumn. On an annual basis, CRU has the lowest absolute values of MBE and RMSE, compared with those of other datasets. However, NOAA shows a smaller error in autumn and winter. In Tianshan Mountains (Region III in Table 1), the correlation coefficients between CRU and observations are higher than those between other datasets and observations on an annual basis. For each season, CRU does not always have the best correlation with observations, and the lowest RMSE can be found for GPCC on annual and seasonal basis except winter. In Kunlun Mountains (Region V in Table 1), only in winter, the correlation coefficients are more than 0.6. The lowest seasonal RMSE can be seen in NOAA (7.59 mm in winter), but CRU has the lowest RMSE on an annual basis. In Junggar and Tarim–Turpan–Hami Basins (Regions II and IV in Table 1), the lowest RMSE existed in GPCC and NOAA.

Table 1
Correlation coefficients (R) between gridded datasets and observations, and mean bias error (MBE) and root-mean-square error (RMSE) of gridded datasets on a seasonal basis in different subregions of Xinjiang during 1979–2010. (I) Altay Mountains; (II) Junggar Basin; (III) Tianshan Mountains; (IV) Tarim–Turpan–Hami Basin; (V) Kunlun Mountains.

Season	Region	CRU			Delaware			GPCC			NOAA		
		R	MBE (mm)	RMSE (mm)	R	MBE (mm)	RMSE (mm)	R	MBE (mm)	RMSE (mm)	R	MBE (mm)	RMSE (mm)
Annual	I	0.78**	−125.9	151.9	0.51*	−147.1	160.8	0.43	−146.3	159.5	0.48**	−138.1	155.6
	II	0.63**	−26.2	69.5	0.68**	−5.2	56.5	0.54**	−13.8	55.4	0.63**	−11.2	54.6
	III	0.58**	−142.8	171.7	0.53**	−143.6	163.8	0.43**	−140.3	161.4	0.44**	−141.8	168.4
	IV	0.39**	29.3	42.5	0.68**	9.1	25.9	0.72**	1.8	17.3	0.57**	−0.1	21.5
	V	0.40**	−12.0	89.5	0.09	−71.1	101.8	0.08	−73.4	100.3	0.15	−77.8	104.0
Spring	I	0.84**	−26.8	39.4	0.54**	−35.5	43.4	0.43	−37.0	43.8	0.55*	−32.5	42.7
	II	0.71**	−6.2	21.6	0.74**	−0.5	18.9	0.67**	−4.7	17.0	0.71**	−3.0	17.5
	III	0.46**	−8.5	46.2	0.65**	−26.1	39.7	0.54**	−27.6	39.5	0.52**	−27.1	41.8
	IV	0.72**	4.5	11.1	0.79**	3.5	8.3	0.82**	1.3	5.7	0.75**	1.0	6.4
	V	0.36**	29.7	51.2	0.46**	3.2	21.9	0.43**	1.3	21.1	0.54**	1.6	20.3
Summer	I	0.70**	−22.6	52.4	0.27	−64.9	78.8	0.36	−59.8	73.8	0.19	−61.0	76.4
	II	0.54**	−16.4	35.2	0.37**	−5.2	31.7	0.08	−7.1	32.1	0.27**	−3.7	31.1
	III	0.65**	−119.1	130.9	0.42**	−103.4	114.8	0.36**	−94.3	107.2	0.40**	−95.1	112.4
	IV	<0.01	18.2	31.0	0.51**	1.2	16.0	0.60**	−1.1	12.5	0.41**	−1.5	15.4
	V	0.39**	−68.0	84.7	0.09	−71.6	85.8	0.05	−70.9	84.4	0.05	−72.3	86.7
Autumn	I	0.76**	−38.9	44.6	0.59**	−27.6	32.2	0.43	−28.3	33.5	0.61**	−27.3	32.5
	II	0.58**	−5.2	19.9	0.81**	−1.6	12.9	0.76**	−2.9	12.6	0.78**	−4.0	13.3
	III	0.45**	−22.9	35.6	0.61**	−18.9	30.5	0.58**	−20.0	28.1	0.56**	−20.6	30.2
	IV	0.44**	5.6	13.5	0.75**	2.6	7.3	0.82**	0.4	4.3	0.72**	−0.2	5.0
	V	0.46**	−1.3	23.2	0.26**	−8.0	17.4	0.17	−8.4	18.0	0.28**	−10.1	19.1
Winter	I	0.59**	−37.7	54.0	0.75**	−19.2	35.0	0.59**	−21.1	34.7	0.77**	−17.3	32.9
	II	0.62**	1.55	13.9	0.91**	2.0	10.1	0.93**	0.9	7.8	0.92**	−0.5	7.5
	III	0.29**	7.74	18.3	0.73**	4.8	13.0	0.71**	1.6	9.9	0.74**	1.1	9.9
	IV	0.73**	1.0	3.5	0.78**	1.8	3.6	0.83**	1.2	2.3	0.71**	0.6	2.4
	V	0.71**	27.8	35.3	0.58**	5.4	10.0	0.52**	4.5	9.1	0.61**	3.0	7.6

Note: * Statistically significant at the 0.05 level. ** Statistically significant at the 0.01 level.

Fig. 5 shows the spatial distribution of RMSE derived from each datasets on seasonal and annual basis, respectively. RMSE is slightly lower in dry winter than that in humid summer. In winter, RMSE is less than 10 mm in most parts of southern Xinjiang, and less than 20 mm in northern Xinjiang. The largest RMSE in winter is located in Altay Mountains and some parts of western Kunlun Mountains, and RMSE of CRU is the largest of the four datasets. In summer, the spatial distribution of RMSE derived from Delaware, GPCC and NOAA is generally similar to the annual figure, in which RMSE in Altay, Tianshan and Kunlun Mountains shows values above 70 mm. In addition, RMSE in Junggar Basin is usually higher than that in Tarim Basin. RMSE on an annual basis shows higher than in summer, and RMSE of CRU is generally larger than that of other datasets.

As elevation rises, MBE gradually changes from positive to negative, and the absolute value shows increasing trend (Fig. 6). RMSE shows an increasing trend with elevation. There is significant underestimation by the gridded datasets in high altitude regions and overestimation in low altitude regions. The gridded datasets can be more effective in simulating precipitation in low-lying basins, with elevation less than 1500 m (mainly desert and scattered oasis). Specifically, MBE in winter shows larger for the altitudes above 2500 m, and RMSE is similar to MBE. Due to precipitation in summer, MBE (and RMSE) shows a significant decreasing (and increasing) trend with altitude increasing.

3.3. Comparison of interannual changes

Fig. 7 and Table 2 show long-term changes in regionally averaged precipitation in the study region from 1979 to 2010. Significant underestimates can be seen from Fig. 7a and c. In the Kunlun Mountains, the interannual changes of observations cannot be simulated by the gridded precipitation datasets. On an annual basis, the increasing magnitude derived from observations in the mountains regions is usually larger than that in low-lying basins. The trend magnitude in Tianshan Mountains is 2.64 mm per year, which is statistically significant at the 0.01 level. For the gridded datasets, the trend magnitudes (ranging from 1.01 to 1.70 mm per year) are usually lower in Tianshan Mountains. GPCC has the nearest trend magnitude (1.70 mm per year, $p < 0.05$), among the four gridded datasets. Similarly, the trend magnitudes in Altay and Kunlun Mountains are also be underrated in the gridded datasets. However, the changes of precipitation in these basins are all statistically non-significant.

Table 2
Trend magnitude of annual precipitation derived from gridded datasets and observations in Xinjiang during 1979–2010 (Unit: mm/year). (I) Altay Mountains; (II) Junggar Basin; (III) Tianshan Mountains; (IV) Tarim–Turpan–Hami Basin; (V) Kunlun Mountains.

Region	Obs	CRU	Delaware	GPCC	NOAA
I	1.53	−0.15	0.96	1.30	0.67
II	1.03	0.49	1.33	1.81	0.76
III	2.64**	1.05	1.15	1.70*	1.01
IV	0.27	0.21	0.51	0.28	0.18
V	1.45*	0.77	0.19	0.47	0.19

Note: * Statistically significant at the 0.05 level. ** Statistically significant at the 0.01 level.

According to the spatial distribution of observation series in Fig. 8, during the past decades, most areas in Xinjiang have experienced a significant wetting trend on an annual basis, especially for the mountainous regions. The wetting trend in summer is more significant than that in winter. On an annual basis, the tendency of increasing precipitation in Tianshan Mountains can be simulated with most datasets, although the precipitation is generally underrated. However, the changes of precipitation in Kunlun Mountains usually cannot be simulated with these gridded precipitation datasets. In summer, the large trend magnitude in Tianshan Mountains is usually hard to be simulated, and CRU has a very limited area with high magnitude over 10 mm per decade.

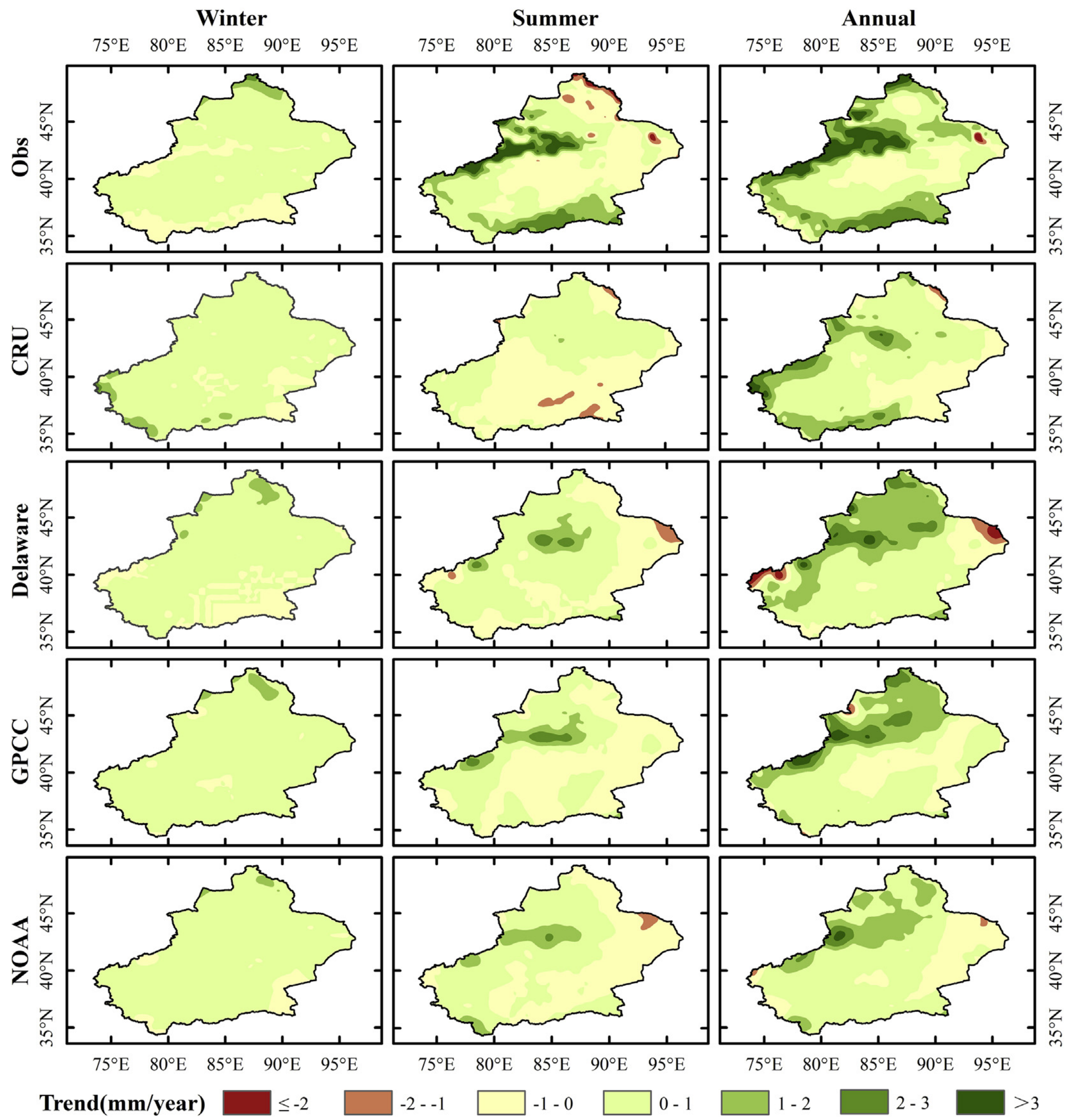

Fig. 8. Spatial distribution of trend magnitude of winter precipitation (left column), summer precipitation (middle column) and annual precipitation (right column) derived from gridded datasets and observations in Xinjiang during 1979–2010.

Fig. 9 shows the correlations of trend magnitude derived from gridded datasets and observations, respectively. The diagonal line indicates $y = x$. Only the boxes with statistical significance in observations are considered in Fig. 9, in order to investigate if the significant trend in observations can be simulated with the gridded datasets. On an annual basis, almost all the points lie at the right-bottom of the diagonal line, indicating these significant increasing trends are generally underrated in the gridded datasets. In winter, a relatively good correlation can be found, compared with the annual series. However, the ranges of trend magnitude are also limited, which is mainly between 0 and 2 mm per year. In summer, the underestimate of gridded datasets is also very significant, especially for CRU (without any significant boxes). Generally, the significant trends derived from gridded datasets are closer to the diagonal line, compared with non-significant trends.

4. Discussion and conclusion

In this study, the reliability of four newly-updated global gridded precipitation datasets with resolution of $0.5° \times 0.5°$ in Xinjiang is investigated. Generally, the main spatial pattern and seasonal variation of precipitation can be simulated by the four gridded precipitation datasets. Precipitation usually is concentrated in summer months, which can be seen from each data source including gridded datasets and observations. Mountainous regions have relatively more precipitation, compared with the surrounding low-lying desert basins, although the relatively humid region in Kunlun Mountains is not well simulated by most gridded datasets.

The precipitation at high elevations is usually underestimated by the gridded datasets, in the Altay, Tianshan and Kunlun Mountains. MBE and RMSE are used to quantify the errors of gridded datasets. Great negative MBE can be found for the mountains, especially for the Tianshan and Altay Mountains. RMSE for the three mountainous regions is more than 40 mm in July, and that for the basin regions is generally lower than 20 mm in January. As altitude increases, the accuracy of gridded precipitation datasets generally decreases. On a seasonal basis, the errors of gridded precipitation datasets in summer months are generally higher than those in other seasons, and RMSE usually shows low values during wintertime.

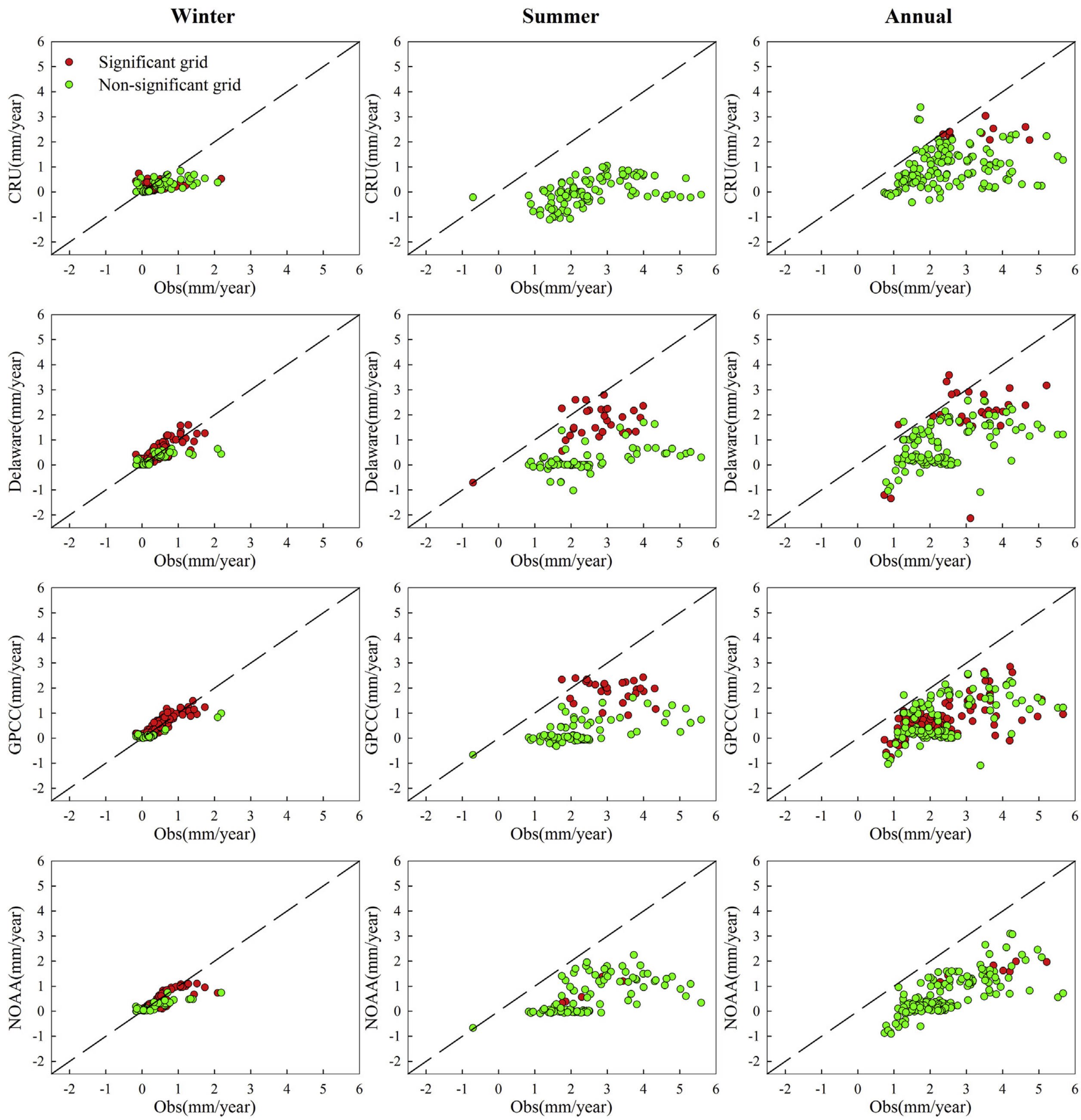

Fig. 9. Correlation of trend magnitude of winter precipitation (left column), summer precipitation (middle column) and annual precipitation (right column) derived from gridded datasets and observations in Xinjiang during 1979–2010. Only the boxes with statistical significance for the observations are shown, and the significance/non-significance of gridded datasets at corresponding boxes is marked in different colors. (For interpretation of the references to colour in this figure legend, the reader is referred to the web version of this article.)

The uneven distribution of the in-situ monitoring network of China Meteorological Administration (CMA) has been widely reported, especially in western China. The great differences of gridded precipitation datasets between mountains and basins are related with the station distribution. For example, there are few automatic meteorological stations in Kunlun Mountains in CMA observation network. The relatively wet climate for this region cannot be supported by the field observations, and cannot be interpolated without consideration of topography. In this study, the Kunlun Mountains usually show significant errors. Similar conditions also exist for all the high altitudes in Xinjiang, although the stations in Tianshan Mountains are more numerous than those in other two mountainous regions. Extremely arid deserts usually have relatively lower errors compared with the mountainous regions. The error of four gridded precipitation datasets presents an increasing trend with altitude, and the simulation is better for the regions below 1500 m a.s.l.

The simulated precipitation derived from CRU is usually far different from other three datasets (Delaware, GPCC and NOAA). Among the four gridded precipitation datasets, RMSE of CRU is slightly larger than those derived from other three datasets in most areas of Xinjiang. These gridded datasets have been widely used in previous investigations, especially CRU (Schiemann et al., 2008; Chen et al., 2011; Huang et al., 2013), and a research using CRU and GPCC shows that annual precipitation in central Asia has increased by 0.62 mm (CRU) and 0.29 mm (GPCC) per decade from 1901 to 2009, respectively (Harris et al., 2014). In spite of the different trend magnitudes derived from different gridded datasets has been shown in this paper, all the increasing rates are underrated. In order to acquire scientific knowledge of long-term precipitation trend using gridded datasets, comparison with observations is needed. Because of the different procedures of data interpolation and/or assimilation, the mean and trend magnitude derived from gridded datasets should be treated with caution.

Acknowledgments

This study was supported by the National Natural Science Foundation of China (No. 41161012) and the National Basic Research Program of China (973 Program) (No. 2013CBA01801).

References

Becker, A., Finger, P., Meyer-Christoffer, A., Rudolf, B., Schamm, K., Schneider, U., Ziese, M., 2013. A description of the global land-surface precipitation data products of the global precipitation climatology centre with sample applications including centennial (trend) analysis from 1901-present. Earth System Science Data 5, 71–99.

Beniston, M., Stephenson, D.B., 2004. Extreme climatic events and their evolution under changing climatic conditions. Global and Planetary Change 44, 1–9.

Bosilovich, M.G., Chen, J., Robertson, F.R., Adler, R.F., 2008. Evaluation of global precipitation in reanalyses. Journal of Applied Meteorology & Climatology 47, 2279–2299.

Bothe, O., Fraedrich, K., Zhu, X., 2012. Precipitation climate of Central Asia and the large-scale atmospheric circulation. Theoretical and Applied Climatology 108, 345–354.

Chen, F.H., Huang, W., Jin, L.Y., Chen, J.H., Wang, J.S., 2011. Spatiotemporal precipitation variations in the arid Central Asia in the context of global warming. Science China Earth Sciences 54, 1812–1821.

Chen, M., Xie, P., Janowiak, J.E., Arkin, P.A., 2002. Global land precipitation: a 50-yr monthly analysis based on gauge observations. Journal of Hydrometeorology 3, 249–266.

Deng, M., Wang, S., Dong, X., et al., 2005. Water Resources and Sustainable Utilization in Xinjiang Uygur Autonomous Region. China Water & Power Press, Beijing (in Chinese).

Harris, I., Jones, P.D., Osborn, T.J., Lister, D.H., 2014. Updated high-resolution grids of monthly climatic observations - the CRU TS3.10 Dataset. International Journal of Climatology 34, 623–642.

Huang, W., Chen, F.H., Feng, S., Chen, J.H., Zhang, X.J., 2013. Interannual precipitation variations in the mid-latitude Asia and their association with large-scale atmospheric circulation. Chinese Science Bulletin 58, 3962–3968.

Isotta, F.A., Frei, C., Weilguni, V., Perčec Tadić, M., Lassègues, P., Rudolf, B., Pavan, V., Cacciamani, C., Antolini, G., Ratto, S.M., Munari, M., Micheletti, S., Bonati, V., Lussana, C., Ronchi, C., Panettieri, E., Marigo, G., Vertačnik, G., 2014. The climate of daily precipitation in the Alps: development and analysis of a high-resolution grid dataset from pan-Alpine rain-gauge data. International Journal of Climatology 34, 1657–1675.

Janowiak, J.E., Gruber, A., Kondragunta, C.R., Livezey, R.E., Huffman, G.J., 1998. A comparison of the NCEP-NCAR reanalysis precipitation and the GPCP rain gauge-satellite combined dataset with observational error considerations. Journal of Climate 11, 2960–2979.

Kistler, R., Kalnay, E., Collins, W., Saha, S., White, G., Woollen, J., Chelliah, M., Ebisuzaki, W., Kanamitsu, M., Kousky, V., Van den Dool, H., Jenne, R., Fiorino, M., 2001. The NCEP-NCAR 50-year reanalysis: monthly means CD-ROM and documentation. Bulletin of the American Meteorological Society 82, 247–267.

Lin, R., Zhou, T., Qian, Y., 2014. Evaluation of global monsoon precipitation changes based on five reanalysis datasets. Journal of Climate 27, 1271–1289.

Ling, H., Xu, H., Fu, J., Zhang, Q., Xu, X., 2012. Analysis of spatial-temporal variation characteristics of extreme air temperature in Xinjiang, China. Quaternary International 282, 14–26.

Ma, L., Zhang, T., Frauenfeld, O.W., Ye, B., Yang, D., Qin, D., 2009. Evaluation of precipitation from the ERA-40, NCEP-1, and NCEP-2 reanalyses and CMAP-1, CMAP-2, and GPCP-2 with ground-based measurements in China. Journal of Geophysical Research: Atmospheres 114, D09105. http://dx.doi.org/10.1029/2008JD011178.

NMIC (National Meteorological Information Center), 2012. Assessment Report of China's Ground Precipitation 0.5°×0.5° Gridded Dataset (V2.0). NMIC, Beijing (in Chinese).

Qian, W., Fu, J., Yan, Z., 2007. Decrease of light rain events in summer associated with a warming environment in China during 1961-2005. Geophysical Research Letters 34. http://dx.doi.org/10.1029/2007GL029631.

Ren, Z., Zhang, M., Wang, S., Qiang, F., Zhu, X., Dong, L., 2015. Changes in daily extreme precipitation events in South China from 1961 to 2011. Journal of Geographical Sciences 25, 58–68.

Schiemann, R., Lüthi, D., Vidale, P.L., Schär, C., 2008. The precipitation climate of Central Asia - intercomparison of observational and numerical data sources in a remote semiarid region. International Journal of Climatology 28, 295–314.

Schneider, U., Becker, A., Finger, P., Meyer-Christoffer, A., Ziese, M., Rudolf, B., 2014. GPCC's new land surface precipitation climatology based on quality-controlled in situ data and its role in quantifying the global water cycle. Theoretical and Applied Climatology 115, 15–40.

Sen, P.K., 1968. Estimates of the regression coefficient based on Kendall's tau. Journal of the American Statistical Association 63, 1379–1389.

Shi, Y., Sun, Z., Yang, Q., 2008. Characteristics of area precipitation in Xinjiang region with its variations. Journal of Applied Meteorological Science 19, 326–332 (in Chinese).

Shiu, C.-J., Liu, S.C., Fu, C., Dai, A., Sun, Y., 2012. How much do precipitation extremes change in a warming climate? Geophysical Research Letters 39, L17707. http://dx.doi.org/10.1029/2012GL052762.

Silva, V.B.S., Kousky, V.E., Higgins, R.W., 2011. Daily precipitation statistics for South America: an intercomparison between NCEP reanalyses and observations. Journal of Hydrometeorology 12, 101–117.

Sohn, S.-J., Tam, C.-Y., Ashok, K., Ahn, J.-B., 2012. Quantifying the reliability of precipitation datasets for monitoring large-scale East Asian precipitation variations. International Journal of Climatology 32, 1520–1526.

Sylla, M.B., Giorgi, F., Coppola, E., Mariotti, L., 2013. Uncertainties in daily rainfall over Africa: assessment of gridded observation products and evaluation of a regional climate model simulation. International Journal of Climatology 33, 1805–1817.

Takahashi, K., Yamazaki, N., Kamahori, H., 2006. Trends of heavy precipitation events in global observation and reanalysis datasets. SOLA 2, 96–99.

Tong, K., Su, F., Yang, D., Zhang, L., Hao, Z., 2014. Tibetan Plateau precipitation as depicted by gauge observations, reanalyses and satellite retrievals. International Journal of Climatology 34, 265–285.

Wang, B., Zhang, M., Wei, J., Wang, S., Li, S., Ma, Q., Li, X., Pan, S., 2013a. Changes in extreme events of temperature and precipitation over Xinjiang, northwest China, during 1960-2009. Quaternary International 298, 141–151.

Wang, H., Chen, Y., Chen, Z., 2013b. Spatial distribution and temporal trends of mean precipitation and extremes in the arid region, northwest of China, during 1960-2010. Hydrological Processes 27, 1807–1818.

Wang, S., Zhang, M., Sun, M., Wang, B., Huang, X., Wang, Q., Feng, F., 2014. Comparison of surface air temperature derived from NCEP/DOE R2, ERA-Interim, and observations in the arid northwestern China: a consideration of altitude errors. Theoretical and Applied Climatology. http://dx.doi.org/10.1007/s00704-014-1107-1.

Wang, S., Zhang, M., Sun, M., Wang, B., Li, X., 2013c. Changes in precipitation extremes in alpine areas of the Chinese Tianshan Mountains, central Asia, 1961-2011. Quaternary International 311, 97–107.

Willmott, C.J., Robeson, S.M., 1995. Climatologically aided interpolation (CAI) of terrestrial air temperature. International Journal of Climatology 15, 221–229.

Xu, W., Li, Q., Wang, X., Yang, S., Cao, L., Feng, Y., 2013. Homogenization of Chinese daily surface air temperatures and analysis of trends in the extreme temperature indices. Journal of Geophysical Research: Atmospheres 118, 9708–9720.

Zhao, T., Fu, C., 2006. Comparison of products from ERA-40, NCEP-2, and CRU with station data for summer precipitation over China. Advances in Atmospheric Sciences 23, 593–604.

Zhao, Y., Zhu, J., Xu, Y., 2014. Establishment and assessment of the grid precipitation datasets in China for recent 50 years. Journal of the Meteorological Sciences 34, 414–420 (in Chinese).

Zolina, O., Simmer, C., Gulev, S.K., Kollet, S., 2010. Changing structure of European precipitation: longer wet periods leading to more abundant rainfalls. Geophysical Research Letters 37. http://dx.doi.org/10.1029/2010GL042468.